

Feasibility analysis of a class of high-order sliding-mode differentiators for redox flow batteries parameter estimation

*¹Pedro Fornaro, ²Thomas Puleston, ¹Paul Puleston, ²Maria Serra-Prat, ²Ramon Costa-Castelló, ¹Pedro Battaiotto

¹*Instituto LEICI, Facultad de Ingeniería, UNLP-CONICET-Asoc.CICPBA*

²*Institut de Robòtica i Informàtica Industrial, CSIC-UPC*

*pedro.fornaro@ing.unlp.edu.ar

Abstract—This work presents the preliminary findings of a feasibility study for a class of sliding mode differentiators to be used in an on-line parameter estimation methodology for vanadium redox flow batteries (VRFB). Specifically, three high-order continuous differentiators are considered: a Standard Differentiator; a Filtering Differentiator, which excels the former by incorporating rejection to large noises small in average; and a Tracking Filtering Differentiator, which produces smooth consistent derivatives while inheriting the noise rejection capabilities from the previous one.

To model the vanadium redox flow batteries an equivalent circuit model is employed, whose time-varying parameters are estimated by a recursive least squares algorithm with forgetting factor, that requires the VRFB measured voltage and current, together with their derivatives. To assess the performance of the different differentiation algorithms in obtaining reliable values of the VRFB parameters, the storage system is excited with standardised current demand profiles. Finally, representative simulation results are presented and discussed.

Index Terms—Vanadium redox flow battery, Sliding mode differentiators, Parameter estimation.

I. INTRODUCTION

The gradual depletion of fossil fuels deposits, together with the impact that their massive utilisation has provoked on the environment has prompted a deployment of carbon-free sustainable energy sources. However, due to the inherent intermittent nature of most major renewable energy sources, such as wind or solar, they still comprise only a minority of the primary power sources. To achieve a greater degree of renewables penetration, they need to be coupled with efficient energy storage systems (ESS) that collect a part of the harvested energy, and deliver it when required [1].

Among the different ESS developed up to now, vanadium redox flow batteries (VRFB) are probably one of the most promising for large scale stationary applications. They gather unique features such as high efficiency, module scalability, independence between capacity and power output, safe and environmentally friendly operation, and long life-time in comparison with other battery technologies [2]. Additionally, the fact that the energy is stored in tanks of electrolyte decoupled from the electrochemical device make it possible for them to be refuelled as quickly as gasoline. As a result, there are ongoing efforts to develop RFB with high energy densities so that they can be competitive also in mobile applications. In this framework, the interest they have raised is so high that there already are some proposals for their implementation in vehicles that do not require long autonomy such as urban electric buses [3].

To fulfil the necessities of a variety of applications, an adequate modelling and a subsequent VRFB characterisation are required. This would permit to rapidly detect failures as well as to improve the control design aiming to optimise their efficiency and satisfy specific power demands. Regarding the VRFB modelling, in this work an equivalent electric circuit model (ECM) is employed [4]. These models have gained a lot of interest and popularity amidst

battery management system designers due to their simplicity in the implementation and relatively low computational cost, particularly when compared to the more complex electrochemical, neural, or distributed parameter models. Specifically, in this work a second order ECM is employed (See Figure 1). With respect to the estimation method utilised to determine the values of the electric elements of the ECM, in this paper a structure based on the combination of sliding mode differentiators (SMD) and a recursive least squares (RLS) with forgetting factor is proposed [5] [6]. This approach requires precise robust information of the voltages and currents of the VRFB and their derivatives. The computation of the latter is not a simple task and, furthermore, the differentiation accuracy normally diminishes together with the order of the required derivatives.

Considering the mentioned aspects, in this work a feasibility analysis of sliding mode based differentiators applied to the estimation method [5] is made. Specifically, among a variety of SMD (e.g. [7]–[12]), three different continuous time differentiators are considered: firstly the so called standard-SMD (SSMD), then the filtering-SMD (FSMD), and finally the tracking-FSMD (TSMD) [13].

II. DESCRIPTION OF THE REDOX FLOW BATTERY MODEL AND PARAMETER ESTIMATION METHODOLOGY

In this section, the VRFB time-varying equivalent circuit model is introduced, along with a brief description of its parameters and associated dynamic equations. Subsequently, the employed estimation method, based on RLS with forgetting factor, is presented.

A. Vanadium redox flow battery equivalent circuit model

In this subsection the ECM of the VRFB is presented (Fig. 1). All parameters are assumed to be slowly time-varying but, for conciseness, the temporal argument t will be omitted in the mathematical formulations.

The open circuit voltage of the battery, v_{oc} , is modelled with the series of a constant source, that corresponds to its minimum value (V_0) and a capacitor C_{bat} , whose electrical charge accounts for the available charge stored in the VRFB. The capacitor varies with the State of Charge (SoC) such that $C_{bat} = \partial Q / \partial v_{oc} = \frac{FQM}{2RTN} (1 - SoC)SoC$, in accordance with the VRFB Nernst equation (for details, see [2]). A series resistance (R_{ohm}) is included to represent the ohmic effects of the membrane, the electrolyte, the porous electrodes and the collector plates. The circuit is completed with a RC module ($R_{pol}-C_{pol}$) to represent the concentration and activation polarisation of the VRFB [4].

• Dynamic equations of the vanadium redox flow battery

The dynamic equations of the VRFB are straightforwardly obtained from the ECM of Figure 1 employing $v_{oc} = V_0 + v_{bat}$, and v_{pol} as

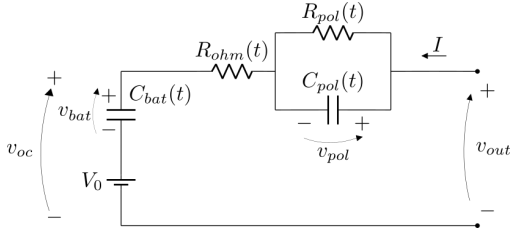


Figure 1. VRFB Electric Equivalent Circuit Model.

the system states. Defining I and v_{out} as the terminal current and voltage of the battery, then:

$$\begin{cases} \dot{\mathbf{v}} = \mathbf{A}\mathbf{v} + \mathbf{B}I = \\ \begin{bmatrix} \dot{v}_{oc} \\ \dot{v}_{pol} \end{bmatrix} = \begin{bmatrix} 0 & 0 \\ 0 & -1/(R_{pol}C_{pol}) \end{bmatrix} \begin{bmatrix} v_{oc} \\ v_{pol} \end{bmatrix} + \begin{bmatrix} \frac{1}{C_{bat}} \\ \frac{1}{C_{pol}} \end{bmatrix} I \\ v_{out} = \mathbf{C}\mathbf{v} + \mathbf{D}I = [1 \quad 1] \begin{bmatrix} v_{oc} \\ v_{pol} \end{bmatrix} + [R_{ohm}] I \end{cases} \quad (1a) \quad (1b)$$

To perform the parameter estimation, the system is described in the Generalised Fliess Canonical Form as presented below. In this representation, the new states are defined as the successive derivatives of the system output: $z_1 = v_{out}$, $z_2 = \dot{z}_1 = \dot{v}_{out}$. The resulting diffeomorphism Φ is:

$$\mathbf{z} = \Phi(\mathbf{v}, I, \dot{I}) = \begin{bmatrix} z_1 \\ z_2 \end{bmatrix} = \begin{bmatrix} \mathbf{C} \\ \mathbf{C}\mathbf{A} \end{bmatrix} \begin{bmatrix} v_{oc} \\ v_{pol} \end{bmatrix} + \begin{bmatrix} \mathbf{D} \\ \mathbf{C}\mathbf{B} + \dot{\mathbf{D}} \end{bmatrix} I + \begin{bmatrix} \mathbf{0} \\ \mathbf{D} \end{bmatrix} \dot{I} \quad (2)$$

and the transformed dynamic system:

$$\begin{cases} \dot{z}_1 = z_2 & (3a) \\ \dot{z}_2 = m_1 \ddot{I} + m_2 \dot{I} + m_3 I + m_4 z_2 & (3b) \\ v_{out} = z_1 & (3c) \end{cases}$$

It can be appreciated that Equation (3b) is linear in the parameters m_1 to m_4 . Then, assuming that these are slow time-varying for almost all t , the terms related to their time derivatives can be neglected. Subsequently, the following relations between the electrical and the new parameters are obtained:

$$m_1 = R_{ohm} \quad (4a)$$

$$m_2 = \frac{1}{C_{bat}} + \frac{1}{C_{pol}} + \frac{R_{ohm}}{C_{pol}R_{pol}} \quad (4b)$$

$$m_3 = \frac{1}{C_{bat}C_{pol}R_{pol}} \quad (4c)$$

$$m_4 = -\frac{1}{C_{pol}R_{pol}} \quad (4d)$$

B. Estimation methodology and real-time results validation

This subsection presents the parameter estimation methodology previously developed in [5] and [6]. This methodology permits to estimate, with a prescribed convergence time and known error bound, the electric parameters of the ECM. To meet this goal, a Recursive Least Square (RLS) with forgetting factor estimation is implemented. This algorithm is utilised to perform a linear regression on (3b), thereby obtaining an estimation of the parameters m_1 to m_4 . Subsequently, the electric parameters and the system states can be straightforwardly obtained by computing the inverse of (4) and (2), respectively. Firstly, before presenting the employed RLS algorithm,

for conciseness sake, the auxiliary equation (3b) is rewritten as follows:

$$\begin{aligned} \eta(t) &= \dot{z}_2 = \ddot{v}_{out} = \boldsymbol{\theta}(t)^\top \boldsymbol{\varphi}(t) = \\ &= [m_1 \quad m_2 \quad m_3 \quad m_4] [\ddot{I} \quad \dot{I} \quad I \quad z_2]^\top \end{aligned} \quad (5)$$

where $\boldsymbol{\varphi}(t) \in \mathbb{R}^4$ is the linear regressor and $\boldsymbol{\theta} \in \mathbb{R}^4$ contains the desired parameters. Thereafter, defining $\hat{\boldsymbol{\theta}}(t)$ as the vector that contains the estimates, the recursive expression that provides the estimation is given by [14]:

$$\dot{\hat{\boldsymbol{\theta}}}(t) = -\mathbf{G} [\mathbf{R}(t)\hat{\boldsymbol{\theta}}(t) + \mathbf{r}(t)] \quad (6)$$

$$\dot{\mathbf{R}}(t) = -q\mathbf{R}(t) + \hat{\boldsymbol{\varphi}}(t)\hat{\boldsymbol{\varphi}}^\top(t) \quad (7)$$

$$\dot{\mathbf{r}}(t) = -q\mathbf{r}(t) - \hat{\boldsymbol{\varphi}}(t)\hat{\boldsymbol{\eta}}(t) \quad (8)$$

where $\mathbf{r}(t)$ and $\mathbf{R}(t)$ are auxiliary variables initialised in zero: $\mathbf{r}(t_0) = \mathbf{0}_{4 \times 1}$, and $\mathbf{R}(t_0) = \mathbf{0}_{4 \times 4}$. The elements of $\hat{\boldsymbol{\varphi}}(t)$ and $\hat{\boldsymbol{\eta}}(t)$ are obtained from the differentiators. The design parameters are the gain matrix \mathbf{G} and the forgetting factor q , which are defined as follows:

- The forgetting factor q , exponentially weights the measured data, giving more relevance to the recent measures with a time constant $\tau = 1/q$.
- \mathbf{G} is a gain matrix that determines the convergence rate of the estimations. It must be symmetric and positive-definite, and has to be designed so that the dynamic of the estimation process is faster than the variation of the system parameters.

It can be proved that, by appropriately selecting the parameters q and \mathbf{G} , an upper bound for the convergence time is [14]:

$$\begin{aligned} T_e &= \frac{n_\tau}{2 \cdot \lambda_{\min}(\mathbf{G}) \cdot \lambda_{\min}(\mathbf{R}(t))} \leq \\ &\leq \frac{n_\tau}{2 \cdot \lambda_{\min}(\mathbf{G}) \cdot \lambda_{pe}} \end{aligned} \quad (9)$$

valid only if the so called *Estimation Condition* holds:

$$\lambda_{\min}(\mathbf{R}(t)) \geq \lambda_{pe} \quad (10)$$

where $\lambda_{pe} > 0$ and n_τ are design constants. Firstly, λ_{pe} is selected to estimate with enough persistence of excitation (PE) during the on-line application of this algorithm. As the convergence and stability properties of (6)-(8) have been well studied in the literature, in this work the PE is assumed to hold during the interval selected for this particular application. Secondly, regarding n_τ , in this paper an accuracy of at least a 95% in the parameter estimation in $T_e = 230s$ employing $n_\tau = 3$ is attained. To the interested reader, the problems related to the measurement of the PE during on-line applications, as well as further details about the employed estimation method are thoroughly detailed in [5].

III. HIGH-ORDER SLIDING MODE BASED DIFFERENTIATION STRATEGIES

In this section the fundamentals of the three types of continuous high-order sliding mode differentiators are presented: standard (SSMD), filtering (FSMD), and tracking (TSMD). A brief description presenting the most relevant aspects of each differentiator is developed.

The three differentiators are capable of robustly provide in finite time asymptotically optimal estimates of a base signal $f(t)$ and its first and second-order derivatives [15] [13] [16] [17]. Furthermore, the estimations are to be exact in the absence of measuring noise. Also, this is possible as long as there is a known bound for the third derivative of $f(t)$, formally referred to as Lipschitz Constant $L > 0$ of $\ddot{f}(t)$. In this work, L is assumed known, as it can be easily

determined by studying the behaviour and limitations of the electrical variables of the VRFB.

In the proposed estimation methodology, these differentiators have a fundamental role, since they permit to obtain derivatives of the measured current and voltage, which are required to perform the regression from equation (5). The main reason for choosing sliding mode based differentiators lies in their finite time convergence. This is a powerful feature, given that allows to considerably improve the RLS estimation rate bound, specially when compared with linear adaptive schemes. It is particularly remarked that, despite all of them converge in finite time, they do not have the same rejection to undesired signals contained in the base signal to differentiate. Furthermore, the error bound to which they converge is not the same, as detailed in [17].

A. Standard Sliding Mode Differentiators

The structure of a SSMD, utilised to estimate up to second-order derivatives, in its non recursive form is the following [13], [15]:

$$\dot{\mu}_1 = -\lambda_2 L^{1/3} |\mu_1 - f(t)|^{2/3} \text{sign}(\mu_1 - f(t)) + \mu_2 \quad (11)$$

$$\dot{\mu}_2 = -\lambda_1 L^{2/3} |\mu_1 - f(t)|^{1/3} \text{sign}(\mu_1 - f(t)) + \mu_3 \quad (12)$$

$$\dot{\mu}_3 = -\lambda_0 L \text{sign}(\mu_1 - f(t)) \quad (13)$$

being $f(t)$ the signal of interest to be differentiated; and $\lambda_0 = 1.1$, $\lambda_1 = 2.12$ and $\lambda_2 = 2$ fixed gains predefined to guarantee the algorithm convergence as explained in [17]. The outputs are the variables $\mu_1 \rightarrow f(t)$, $\mu_2 \rightarrow \dot{f}(t)$ and $\mu_3 \rightarrow \ddot{f}(t)$. It can be highlighted the capability of the SSMD to provide robust exact derivatives of $f(t)$ in the absence of noise, and asymptotically optimal estimates in the presence of bounded noise, i.e. with a known error bound determined by the noise magnitude [15].

B. Filtering Sliding Mode Differentiators

In spite of the robustness of SSMDs with respect to small bounded noises, their accuracy can be affected by high-value spurious signals that can distort the current and voltage measurements. This is a problem of particular interest in power electronics and in applications such as the presented in this work. To deal with this problem, without compromising its precision, the FSMD includes a sliding mode filter. It is capable to reject large noises small in average, particularly unbounded noises of filtering order not exceeding the differentiator filtering order [17]. The structure of such FSMD in its non-recursive form is the following [17]:

$$\dot{w}_1 = -\lambda_4 L^{1/5} |w_1|^{4/5} \text{sign}(w_1) + w_2 \quad (14)$$

$$\dot{w}_2 = -\lambda_3 L^{2/5} |w_1|^{3/5} \text{sign}(w_1) + (\mu_1 - f(t)) \quad (15)$$

$$\dot{\mu}_1 = -\lambda_2 L^{3/5} |w_1|^{2/5} \text{sign}(w_1) + \mu_2 \quad (16)$$

$$\dot{\mu}_2 = -\lambda_1 L^{4/5} |w_1|^{1/5} \text{sign}(w_1) + \mu_3 \quad (17)$$

$$\dot{\mu}_3 = -\lambda_0 L \text{sign}(w_1) \quad (18)$$

Note that (16) to (18) are somewhat equivalent to those of the SSMD. On the other hand, (14) and (15) constitute a sliding mode filter which in this particular case is of second order. The filter is applied to the difference between the signal to be differentiated and its estimate: $(\mu_1 - f(t))$. After a finite-time transient, the signal w_1 is a filtered version of that difference. The outputs of the differentiator are $\mu_1 \rightarrow f(t)$, $\mu_2 \rightarrow \dot{f}(t)$ and $\mu_3 \rightarrow \ddot{f}(t)$. In this case, the gains λ_i are adjusted as in [17]: $\lambda_0 = 1.1$ $\lambda_1 = 4.57$ $\lambda_2 = 9.30$ $\lambda_3 = 10.03$ y $\lambda_4 = 5$.

It is worth noting that in both SSMD and FSMD the derivatives estimates contain high frequency oscillations inherent to the differentiation structure, generated by the fractional power terms in the

right hand side of (11) to (13) in the SSMD and (16) to (18) in the FSMD case. This phenomenon, normally referred to as *chattering*, is subsequently introduced in the RLS as a high frequency component but does not contain relevant information to the parameter estimation. The effects of the chattering are discussed in section IV.

C. Tracking Sliding Mode Differentiators

The third and last type of sliding mode differentiator analysed in this work is the *tracking* SMD. It possess the same virtues of the FSMD with regard to its capacity to reject large noises small in average. However, TSMD include in their structure a higher order $(n + 1)$ sliding mode control algorithm with the purpose of keeping the sliding mode variable $\sigma = f(t) - \zeta_1$ and its derivatives up to the order n equal to 0. ζ_1 is the estimate of the signal to be differentiated $f(t)$, extracted from a chain of integrators. As in this work $n = 2$, the resulting control objective is: $\sigma = \dot{\sigma} = \ddot{\sigma} = 0$. The structure of a second order TSMD, in its non recursive form is [17]:

$$\dot{w}_1 = -\lambda_4 5 L^{1/5} |w_1|^{4/5} \text{sign}(w_1) + w_2 \quad (19)$$

$$\dot{w}_2 = -\lambda_3 5 L^{2/5} |w_1|^{3/5} \text{sign}(w_1) + (\mu_1 - \sigma) \quad (20)$$

$$\dot{\mu}_1 = -\lambda_2 5 L^{3/5} |w_1|^{2/5} \text{sign}(w_1) + \mu_2 \rightarrow \dot{\hat{\sigma}} = \mu_1 \quad (21)$$

$$\dot{\mu}_2 = -\lambda_1 5 L^{4/5} |w_1|^{1/5} \text{sign}(w_1) + \mu_3 \rightarrow \ddot{\hat{\sigma}} = \mu_2 \quad (22)$$

$$\dot{\mu}_3 = -\lambda_0 5 L \text{sign}(w_1) \rightarrow \hat{\hat{\sigma}} = \mu_3 \quad (23)$$

$$\dot{\zeta}_1 = \zeta_2 \quad (24)$$

$$\dot{\zeta}_2 = \zeta_3 \quad (25)$$

$$\dot{\zeta}_3 = \nu = -4 \frac{\mu_3^3 + |\mu_2|^{3/2} \text{sign}(\mu_2) + \mu_1}{|\mu_3|^3 + |\mu_2|^{3/2} + |\mu_1|} \quad (26)$$

Observe that the structure of (19) to (23) is equivalent to that of the FSMD. Indeed, these equations comprise a second order differentiator to compute derivatives of the sliding surface σ . Besides, $\dot{\zeta}_3$ is defined utilising the estimates of the sliding variable derivatives μ_1 , μ_2 and μ_3 , in order to develop a control action ν that guarantees $\sigma = \dot{\sigma} = \ddot{\sigma} = 0$. The outputs of this scheme are the parameters $\zeta_{1,2,3}$, obtained from the chain of integrators (24)-(26). As a result, the derivative estimates are smooth and consistent, i.e. each estimated derivative is the integral of the following: $\dot{\zeta}_1 = \zeta_2$ and $\dot{\zeta}_2 = \zeta_3$.

As presented in [17], the TSMD estimation accuracy of $|\zeta_i - f^{(i)}|$ are of the order $|f(t)^{(i+1)}|$ independently of noises and sampling periods. However, their consistency turns out to be of vital importance in estimation algorithms, and the feasibility of these differentiators in our particular application is therefore thoroughly evaluated. Indeed, as will be discussed in the results section, the performance of the estimation algorithm heavily relies on the quality of the input variables conforming the regressor vector.

IV. RESULTS AND DISCUSSION

This section presents and analyses representative results of the simulations obtained in the Matlab Simulink® environment. In this sense, the performance of the previously presented differentiation algorithms is compared and contrasted, in particular with regard to their application to the estimation of the parameters m_i of equation (3b).

To perform a valid comparison between these algorithms, sampling step of $2.5e^{-5}$ s is utilised. The estimation results are calculated by conforming the regressor (5) and η with the estimated derivatives obtained from the SSMD, FSMD and TSMD, respectively. To this end, the Lipschitz constants are set $L_v = 250$ and $L_i = 700$ for the differentiators to compute the voltage and the current derivatives. As for the estimation parameters setup please refer to [18].

A comprehensive analysis involving a large number of tests with different levels of noise was made. For the sake of space, only two representative sets of these results are presented and discussed in this work. The first set was performed in an ideal noise-free scenario. The second one included additive noise to study the robustness of the proposed methodology when the differentiators are subjected to more exigent conditions. Note that, in those cases where the accuracy of the estimation is very high, some of the resulting curves corresponding to the different differentiators may be overlapped.

To simulate an on-line estimation environment, it is assumed that the VRFB operates under a variable current demand profile, generated using a standardised urban driving profile. The main reasons to employ this profile are twofold. On the one hand, it is a current demand profile with enough PE, therefore simplifies the results comprehension. On the other hand, as previously mentioned, even though it still requires further studies and improvements, the utilisation of VRFB in vehicular applications is an attractive alternative to standard batteries. The current profile, together with the resulting output voltage obtained with the ECM are shown in Figure 2.

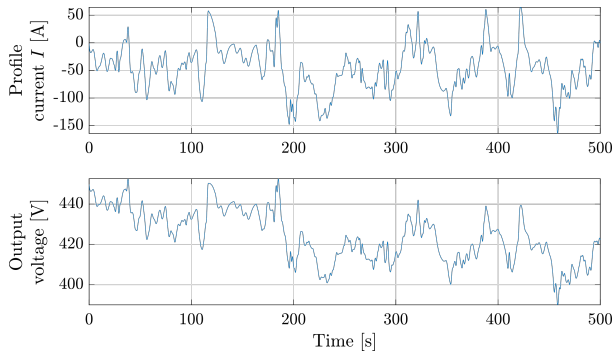


Figure 2. (Up) Current profile. (Bottom) Output VRFB voltage.

A. Results comparison employing SSMD and FSMD

In this subsection, the results of the parameter estimation obtained by employing SSMD and FSMD are compared and analysed. When the signals to be differentiated are free of noise, the estimation performance is very similar for both differentiators (see Fig. 3). This is because the accuracy asymptotics of both SSMD and FSMD is preserved. To better visualise the obtained results, the relative error is computed and shown in Fig. 5. It can be appreciated that, in both cases, after an initial convergence lapse, the relative error stays below 5% for all the parameters.

Subsequently, to assess the advantages of including a sliding mode filter in the differentiation algorithm, a second simulation is performed (see Fig. 4). In this case, white noise was introduced in the measured signals I and v_{out} . Additionally, a high frequency component $\epsilon = 0.01 \sin(10000t)$ was also included, aiming to put the algorithms under even more challenging conditions. In this scenario, the estimates obtained with the SSMD are seriously affected, with an error that surpasses 20% in the estimation of m_3 (See Fig. 6). Conversely, the FSMD performs considerably better, with its relative error being less than half the SSMD's error.

B. Results comparison employing FSMD and TSMD

To perform a comparative analysis between the FSMD and the TSMD, it is firstly highlighted that both algorithms inherently possess the same capabilities to reject undesired noises contained in the base signal.

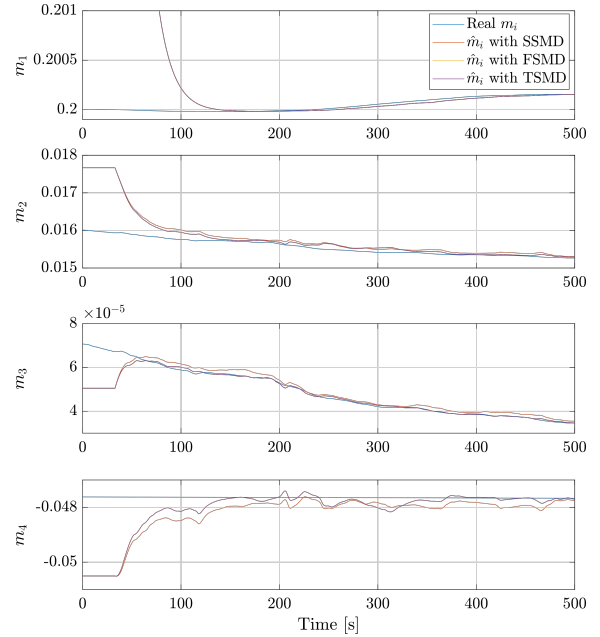


Figure 3. Estimated parameters without additive noise employing SSMD, FSMD and TSMD.

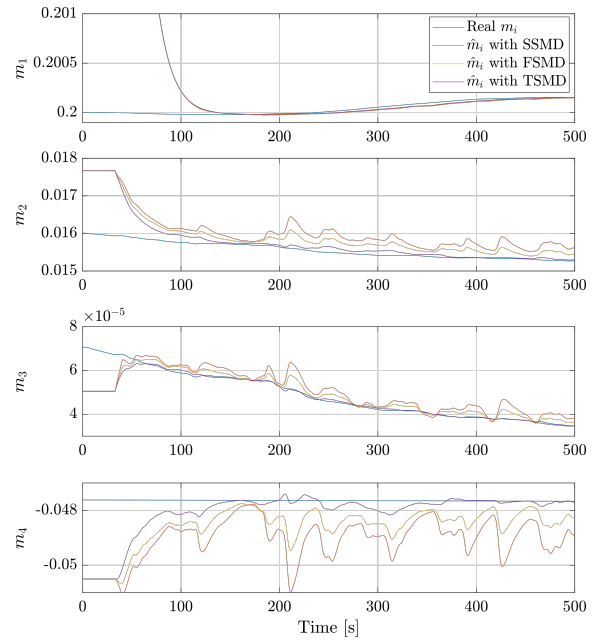


Figure 4. Estimated parameters with additive noise employing SSMD, FSMD and TSMD.

To understand the incidence of each differentiator on the parameter estimation process, it is initially of interest to analyse the current error $(I - \hat{I})$ and the first derivative error $(\dot{I} - \hat{\dot{I}})$ without noise (See Fig. 7). In the first place, observe that the error in the estimates is exiguous in both differentiators. However, note that the amplitude of the TSMD error is considerably higher than the one of the FSMD. On the other hand, the derivatives of the TSMD are smoother and consistent, since they are obtained from a chain of integrators.

Then, even though both the FSMD and the TSMD possess the same noise rejection capabilities, the smoothness and consistency of the

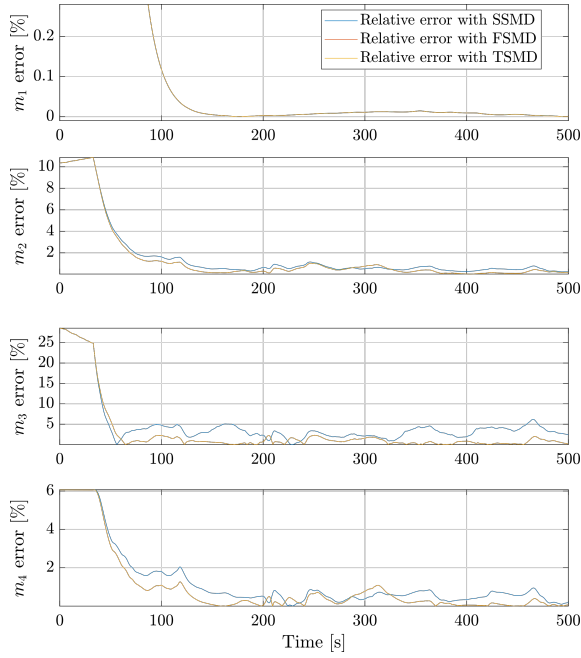


Figure 5. Relative error comparison [%] in the parameter estimation employing SSMD, FSMD and TSMD without additive noise in the differentiated signals.

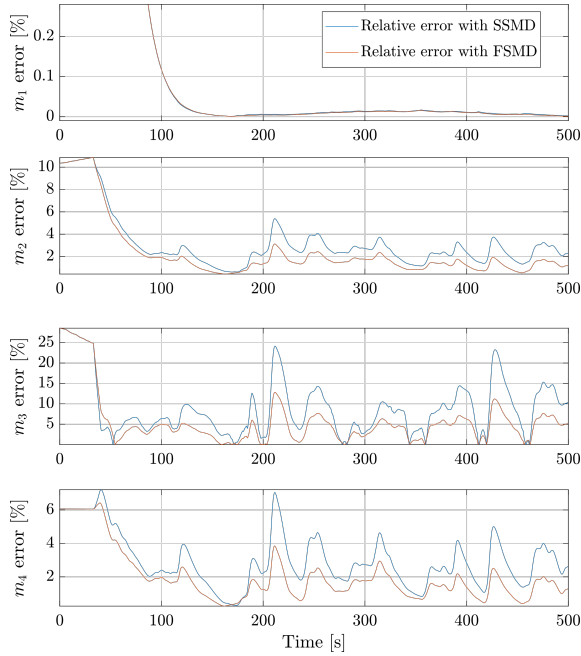


Figure 6. Relative error comparison [%] in the parameter estimation employing SSMD and FSMD with additive noise in the differentiated signals.

TSMD derivatives is a determinant factor to improve the estimation. This can be appreciated in Figs. 5 and 8 where, with or without noise, the relative error in the RLS estimation is maintained below a %5 error bound. For its part, under exacting noise conditions, the use of the FSMD still provides an acceptable estimation error, although accuracy is worsen in comparison to the TSMD.

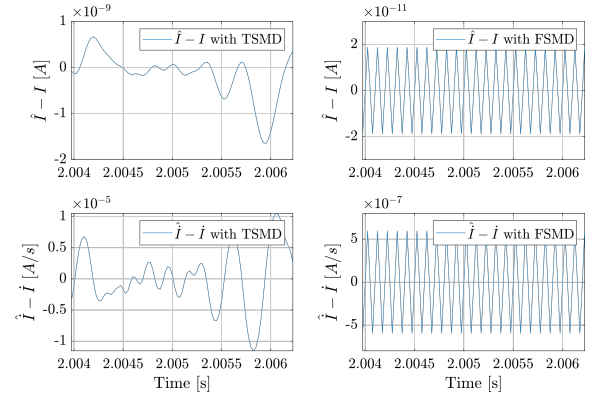


Figure 7. Error in the current (I) and derivative (\dot{I}) estimation employing TSMD (left) and FSMD (right).

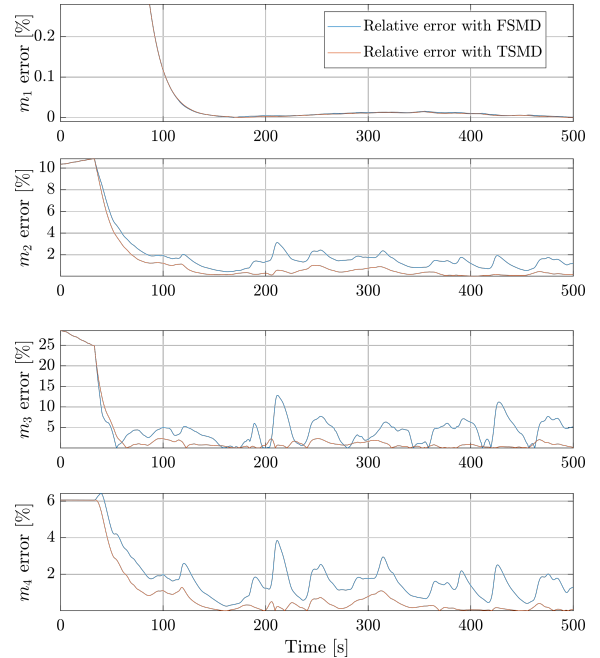


Figure 8. Relative error comparison [%] in the parameter estimation employing FSMD and TSMD with additive noise in the differentiated signals.

V. CONCLUSIONS

The work presented in this paper was undertaken as part of a project aiming to develop an estimation methodology to deal with energy storage systems utilised in sustainable hybrid energy systems. In this stage, three differentiators were evaluated to be applied in on-line estimation of VRFB parameters: a Standard, a Filtering and a Tracking SMD.

Without (or with very low) noise, all of them demonstrated excellent behaviours, allowing finite-time convergence for the regression equation variables which, in the VRFB under study, are the voltage, the current and their respective time derivatives. Above a certain level of noise the performance of the Standard SMD visibly deteriorates. Conversely, the Filtering and the Tracking SMDs, keep on delivering very good results. Subsequently, putting them to test under exacting noise conditions, the TSMD proved capability to better deal with it. The results reveal that, even though the error amplitude in the FSMD's derivatives are lower than the ones of the TSMD, the

consistency in the estimated derivatives of the latter positively impact in the parameter estimations.

Therefore, it can be concluded that the Filtering and the Tracking SMDs are both applicable alternatives to implement the RLS with forgetting factor methodology for flow batteries on-line estimation. The latter is recommended, however if a lower computational burden is required, the former is also a highly suitable option.

As future work, other differentiation strategies, as well as different methods for the differentiators discretisation, will be investigated.

ACKNOWLEDGEMENTS

Thanks to the support of the UNLP, CONICET, Agencia I+D+i from Argentina, and "la Caixa" Foundation (ID 100010434. Fellowship code LCF/BQ/DI21/11860023), the UPC, CSIC, MCIN and project PID2021-126001OB-C31 funded by MCIN/ AEI/ 10.13039/501100011033 / ERDF,EU.

REFERENCES

- [1] Q. Xu and T. S. Zhao, "Fundamental models for flow batteries," *Progress in Energy and Combustion Science*, vol. 49, pp. 40–58, 8 2015.
- [2] O. C. Esan, X. Shi, Z. Pan, X. Huo, L. An, and T. S. Zhao, "Modeling and simulation of flow batteries," *Advanced Energy Materials*, 2020.
- [3] L. Barelli, G. Bidini, P. A. Ottaviano, and D. Pelosi, "VRFB application to electric buses propulsion: Performance analysis of hybrid energy storage system," *Journal of Energy Storage*, vol. 24, 8 2019.
- [4] Z. Wei, S. Meng, K. J. Tseng, T. M. Lim, B. H. Soong, and M. Skyllas-Kazacos, "An adaptive model for vanadium redox flow battery and its application for online peak power estimation," *Journal of Power Sources*, vol. 344, pp. 195–207, 2017.
- [5] P. Fornaro, P. Puleston, and P. Battaiotto, "On-line parameter estimation of a lithium-ion battery/supercapacitor storage system using filtering sliding mode differentiators," *J. of Energy Storage*, 2020.
- [6] P. Fornaro, P. Puleston, and P. Battaiotto, "Metodología de estimación en tiempo real para un sistema de almacenamiento supercapacitor/batería de ion-litio en vehículos eléctricos," in *AADECA 2020*, 2020.
- [7] G. Bartolini, A. Ferrara, and E. Usai, "Real-time output derivatives estimation by means of higher order sliding modes," in *IMACS Multiconference (CESA'98)*, vol. 1, 1998, pp. 782–787.
- [8] B. Cannas, S. Cincotti, and E. Usai, "An algebraic observability approach to chaos synchronization by sliding differentiators," *IEEE Transactions on Circuits and Systems I: Fundamental Theory and Applications*, vol. 49, no. 7, pp. 1000–1006, jul 2002.
- [9] H. Alwi and C. Edwards, "An adaptive sliding mode differentiator for actuator oscillatory failure case reconstruction," *Automatica*, vol. 49, no. 2, pp. 642–651, feb 2013.
- [10] M. T. Angulo, J. A. Moreno, and L. Fridman, "Robust exact uniformly convergent arbitrary order differentiator," *Automatica*, vol. 49, no. 8, pp. 2489–2495, aug 2013.
- [11] E. Cruz-Zavala, J. A. Moreno, and L. M. Fridman, "Uniform robust exact differentiator," *IEEE Transactions on Automatic Control*, vol. 56, no. 11, pp. 2727–2733, nov 2011.
- [12] R. Seeber, H. Haimovich, M. Horn, L. M. Fridman, and H. De Battista, "Robust exact differentiators with predefined convergence time," *Automatica*, vol. 134, p. 109858, dec 2021.
- [13] A. Levant, "Higher-order sliding modes, differentiation and output-feedback control," *International J. of Control*, vol. 76, 2003.
- [14] G. Kreisselmeier, "Adaptive observers with exponential rate of convergence," *IEEE Trans. on Automatic Control*, vol. 22, 1977.
- [15] A. Levant, "Robust exact differentiation via sliding mode technique," *Automatica*, vol. 34, no. 3, pp. 379–384, mar 1998.
- [16] A. Levant, "Homogeneity approach to high-order sliding mode design," *Automatica*, no. 5, 2005.
- [17] A. Levant and M. Livne, "Robust exact filtering differentiators," *European Journal of Control*, aug 2019.
- [18] P. Fornaro, T. Puleston, P. Puleston, M. Serra, R. Costa, and P. Battaiotto, "Redox flow battery time-varying parameter estimation based on high-order sliding mode differentiators," *Int. j. of Energy research*, 2022.